Chemical Triple-Mutant Boxes for Quantifying Cooperativity in Intermolecular Interactions

Christopher A. Hunter,*[a] Philip S. Jones,[b] Pascale Tiger,[a] and Salvador Tomas[a]

Abstract: Chemical double-mutant cycles have been used to quantify intermolecular functional-group interactions in H-bonded zipper complexes in chloroform. If the same interaction is measured in zippers of different overall stability, the double-mutant cycles can be combined to produce a triple-mutant box. This construct quantifies cooperativity between the functional group interaction of interest and the other interactions that are used to change the overall stability of the complexes. The sum of two edge-to-face aromatic interactions (-2.9 ± 0.5 kJ mol^{-1}) is shown to be insensitive to changes of up to 13.7 ± 0.2 kJ mol^{-1} in the overall stability of the complex. In principle, enthalpic cooperative effects caused by entropy–enthalpy compensation could perturb the measurement of intermolecular interactions when using the double-mutant cycle approach, but these experiments show that, for this system, the magnitude of the effect lies within the error of the measurements.

Keywords: cooperative phenomena · enthalpy–entropy compensation · supramolecular chemistry · weak interactions

Introduction

The characterisation of weak, noncovalent interactions is an issue of fundamental interest in supramolecular and biological chemistry,[1] since these interactions control a range of processes, such as protein folding, molecular recognition and the formation of crystalline solids. If we are to formulate molecular-design strategies based on such processes, a detailed quantitative understanding of intermolecular interactions is essential. One of the most difficult questions to address is the way in which any given interaction is affected by the presence of other nearby interactions, that is, cooperative effects.

The enthalpy of an interaction can be altered by nearby interactions due to a change in conformation or electronic structure. Inductive effects cause a change in internal electronic structure that leads to the cooperative reinforcement of polar interactions such as hydrogen bonds (Figure 1a).[2–8] If a receptor binds two different molecules, cooperativity can be mediated by direct interactions between the two substrates (Figure 1b).[9–15] For a conformationally mobile molecule with several interaction sites, the formation of one binding interaction may affect a subsequent interaction, by altering the accessible conformational states (Figure 1b). This can be manifested in the enthalpy if a high-energy conformation is required for binding, or in the entropy

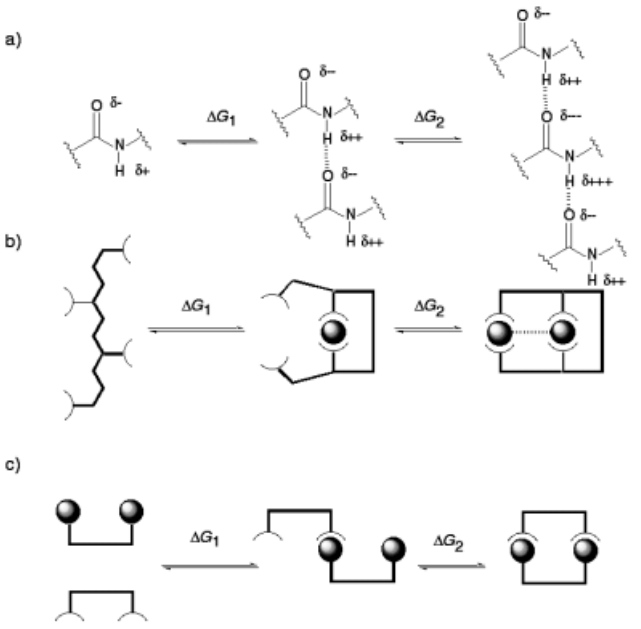

Figure 1. Different forms of cooperativity ($\Delta G_2 \neq \Delta G_1$). a) Cooperativity mediated by a change in electronic structure. b) Cooperativity mediated by a conformational change. c) The classic chelate effect.

[a] Prof. C. A. Hunter, Dr. P. Tiger, Dr. S. Tomas
Centre for Chemical Biology
Krebs Institute for Biomolecular Science, Department of Chemistry
University of Sheffield, Sheffield, S3 7HF (UK)
Fax: (+44) 114-273-8673
E-mail: c.hunter@sheffield.ac.uk

[b] Dr. P. S. Jones
Roche Discovery Welwyn, 40 Broadwater Road
Welwyn Garden City, Hertfordshire, AL7 3AY (UK)

  0947-6539/02/0823-5435 $ 20.00+.50/0

if a flexible molecule must adopt a more organised conformation for binding.[1, 3, 16–21]

The entropy cost of restricting the overall molecular translational and rotational degrees of freedom in an intermolecular association does not apply to an intramolecular interaction (Figure 1c), and this gives rise to cooperativity, generally termed the chelate effect.[22–24] Changes in solvation may also play an important role in mediating cooperative effects, especially with respect to the interplay between the enthalpic and entropic contributions.

When a molecule interacts with a receptor, a significant amount of residual intermolecular motion still remains, and so the entropy lost is generally less than the theoretical maximum. If another intermolecular interaction is now added, the residual intermolecular motion will be restricted, so the favourable enthalpy due to the new interaction will be compensated for to some extent by an entropy loss. Williams has suggested that this gives rise to the commonly observed phenomenon of enthalpy–entropy compensation.[1, 25, 26] There is a finite entropy associated with the intermolecular degrees of freedom that can be lost when a complex is formed. Thus, as intermolecular interactions become more enthalpically favourable, the entropy loss should approach this limit, that is, the compensation between enthalpy and entropy should follow an asymptotic curve rather than a straight line. In practice, this means that maximal chelate effects will only be realised in systems where all of the intermolecular degrees of freedom have already been removed by other interactions.

This has consequences for the enthalpies associated with the individual interactions that hold a complex together. When there is a lot of residual motion in a weakly bound complex, all of the interactions will be weakened compared with a strongly bound complex. Williams has proposed a model based on differences in the shapes of the enthalpic wells in these two situations (Figure 2).[1, 25, 26] Consider a single point interaction between two functional groups i and j. The strongly bound complex (A′) has a deep narrow enthalpic well, and so the thermally populated intermolecular vibrational states sample a very small range of i–j separations (Δx). In contrast, in the weakly bound complex (A), the broad shallow potential well leads to thermal population of many intermolecular vibrational states in which the i–j separation varies over a large amplitude. Thus the mean functional-group separation is larger in a weakly bound complex, and the interaction enthalpy will be correspondingly reduced (by $\Delta\Delta H_{i\text{-}j}$) relative to the maximum value that is observed in strongly bound complexes. Evidence for this enthalpic chelate effect has been obtained from studies of complexes of the vancomycin family of antibiotics with peptides.[1, 3, 4, 20, 27]

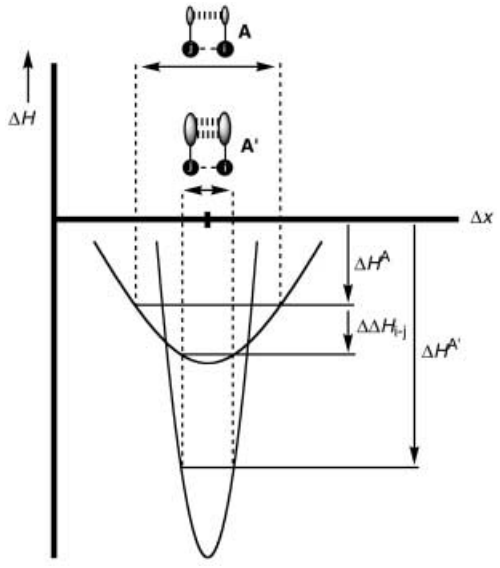

Figure 2. The enthalpic chelate effect. The intermolecular vibrational modes are damped in a strongly bound complex (**A′**) compared with a weakly bound complex (**A**), because the potential well is deeper and narrower. Thus on average, the separation between two interacting groups i and j (Δx) is reduced in a strongly bound complex, and this leads to an increase in the enthalpy of interaction ($\Delta\Delta H_{i\text{-}j}$).

We have been working on the quantification of weak intermolecular functional-group interactions using a chemical version of the double-mutant cycles originally devised to investigate interactions in proteins.[28–36] Entropy–enthalpy compensation has important implications for such studies. If enthalpic chelate effects are large, then any attempts to experimentally quantify intermolecular functional-group interaction energies will be prone to errors, unless the experiments are carried out at the strong binding limit. Conversely, the double-mutant approach for measuring functional group interaction energies provides us with a convenient tool with which to directly probe the magnitude of the enthalpic chelate effect experimentally. Thus chemical double-mutant cycles can be used to measure the magnitude of a particular functional-group interaction in both weakly and strongly bound complexes. Any difference between the functional-group interaction energies in the two systems provides a measure of the magnitude of the enthalpic chelate effect in these complexes.

This kind of approach has been used previously to measure cooperative interactions at protein–protein interfaces.[2, 5, 7, 8] Two double-mutant cycles can be formally combined to produce a triple-mutant box, as illustrated in Figure 3, and this provides a general method for quantifying cooperative effects. Complexes A–D are used to measure the i–j interaction in a weakly bound complex by using the usual double-mutant cycle method, which enables us to dissect out one isolated functional-group interaction from the array of other interactions and secondary effects that contribute to the overall

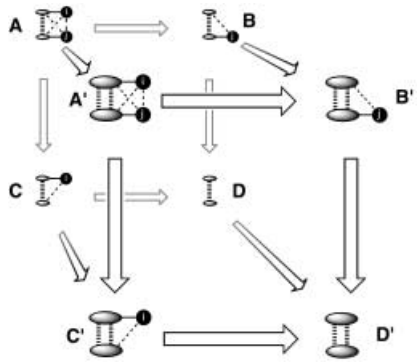

Figure 3. A triple-mutant box for determining the magnitude of the cooperativity between the interaction of two functional groups, i and j, and additional interactions that stabilise the core of the complex.

0947-6539/02/0823-5436 $ 20.00+.50/0 *Chem. Eur. J.* **2002**, *8*, No. 23

binding energy of Complex A (back face of the cube in Figure 3) [Eq. (1)].

$$\Delta\Delta G_{i\text{-}j} = \Delta G_A - \Delta G_B - \Delta G_C + \Delta G_D \quad (1)$$

Complex A′ contains exactly the same i–j interaction in exactly the same environment, but with some additional remote interactions that increase the overall stability of this system relative to Complex A. The double-mutant cycle constructed with Complexes A′–D′ therefore measures the i–j functional-group interaction in the more strongly bound complex, A′ (front face of the cube in Figure 3) [Eq. (2)].

$$\Delta\Delta G'_{i\text{-}j} = \Delta G_{A'} - \Delta G_{B'} - \Delta G_{C'} + \Delta G_{D'} \quad (2)$$

The difference between the two measurements of the i–j interaction is the magnitude of the cooperativity between the additional interactions present in Complex A′ and the i–j interaction [Eq. (3)].

$$\Delta\Delta G_{coop} = \Delta\Delta G'_{i\text{-}j} - \Delta\Delta G_{i\text{-}j} \quad (3)$$

This procedure is clearly based on measurements of free energy rather than enthalpy, but an enthalpic chelate effect must manifest itself as a cooperativity in free energy in this scheme. Thus the triple-mutant box will allow us to directly probe enthalpic cooperativity.

Approach: The system that we have used previously to quantify edge-to-face aromatic interactions is shown in Figure 4.[35] The interaction between the terminal *tert*-butylbenzoyl (**T**) and diisopropyl aniline (**A**) groups was found to be -1.4 ± 0.8 kJ mol^{-1} by mutating **T** to trimethyacetyl (**X**) and **A** to *n*-hexylamine (**H**) and constructing the double-mutant cycle. The cycle in Figure 4 actually measures the sum of the two terminal **T**·**A** interactions, and, to obtain the value above, we have previously assumed that the two interactions have the same energy, but this assumption does not impinge on the triple-mutant analysis presented in this paper. Complex A in Figure 4 is the first member of a family of related zipper complexes that are amide oligomers composed of the alternating repeats of the bisaniline (**B**) and isophthalic acid (**I**) subunits, **TBT**·**AIA**, (**AIBT**)$_2$, **TBIBT**·**AIBIA**, and so on (see Figure 5).[18, 37] These complexes are ideally adapted for the triple-mutant box experiment shown in

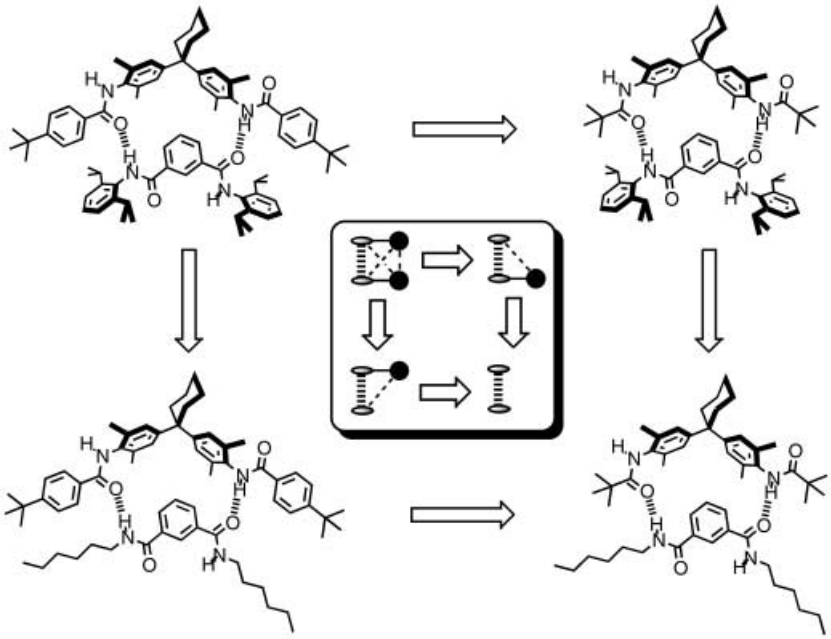

Figure 4. A chemical double-mutant cycle for determining the magnitude of the two terminal edge-to-face interactions in complex A. Inset: the cartoon relationship to Figure 3.

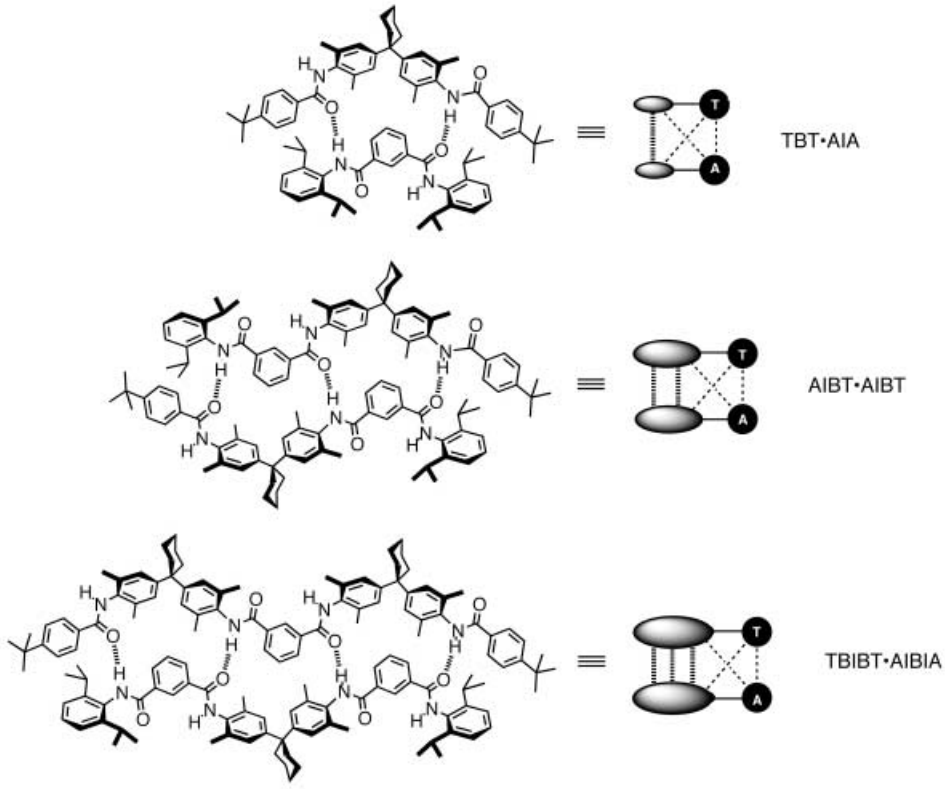

Figure 5. The family of zipper complexes used in this study. The cartoon relationship to Figure 3 is also shown.

  0947-6539/02/0823-5437 $ 20.00+.50/0

Figure 3. The stability of the zipper complex increases by an order of magnitude for every **B·I** subunit added, and intermolecular NOEs together with the complexation-induced changes in ^{1}H NMR chemical shift show that the structures of the terminal **A·T** edge-to-face interactions are essentially identical in these systems. Thus **T**→**X** and **A**→**H** mutations on the zipper complexes in Figure 5 will allow us to construct three triple-mutant boxes: by combining the **TBT·AIA** and (**AIBT**)$_2$, the **TBT·AIA** and **TBIBT·AIBIA**, and the (**AIBT**)$_2$ and **TBIBT·AIBIA** double-mutant cycles.

Results and Discussion

Synthesis: The first problem we faced in implementing this approach was solubility. The longer zipper components are almost insoluble in chloroform. They can be solubilised with small amounts of methanol, but this destabilises the short zipper complexes to the extent that it is not possible to measure accurate binding constants. We therefore developed an analogue of the bisaniline building block equipped with a site for the attachment of solubilising groups (Scheme 1). The compound 2,6-dimethylaniline was heated under reflux with piperidin-4-one and HCl to give the piperidine analogue of H_2N-**B**-NH_2, **1**. Condensation of the secondary amine with benzylchloroformate gave H_2N-**B^1**-NH_2. Amide oligomers incorporating this subunit showed significantly improved solubility, but the carbobenzoxy (Cbz) group was not sufficient to solubilise **AIBIA** or the associated mutant **XIBIX**. For these compounds, the gallic acid derivative **2** shown in Scheme 1 was required in order to achieve good solubility in pure chloroform. The fact that solubilising groups are different in different classes of compound does not affect the thermodynamic analysis, since all four complexes in every double-mutant cycle have an identical set of solubilising groups.

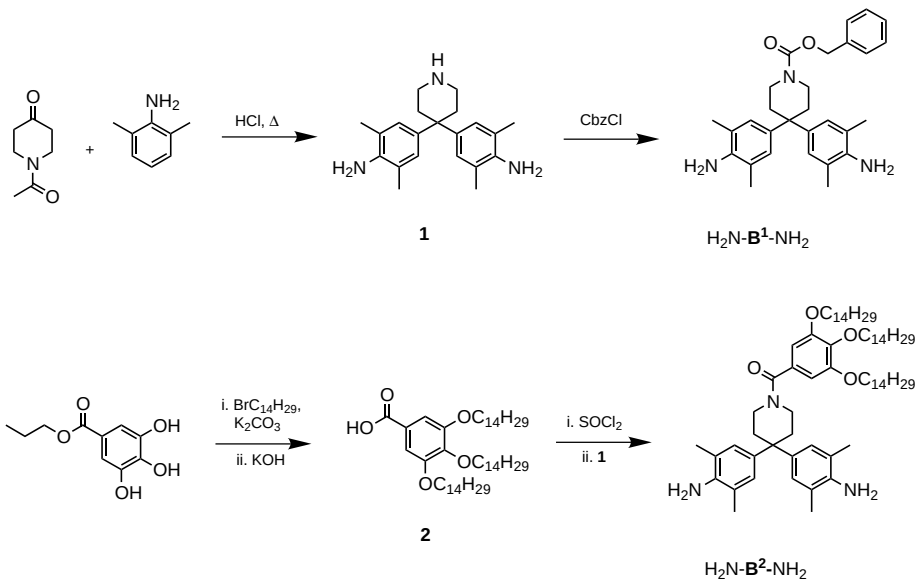

Scheme 1.

The components of the shortest zippers based on **AIA·TBT** were obtained in a straightforward fashion by single-step coupling reactions. The syntheses of **AIA** and **HIH** have been described previously.[37, 38] **TB^{1}T** and **XB^{1}X** were obtained by treating H_2N-**B^1**-NH_2 with an excess of 4-*tert*-butylbenzoyl chloride or trimethylacetyl chloride respectively (Scheme 2).

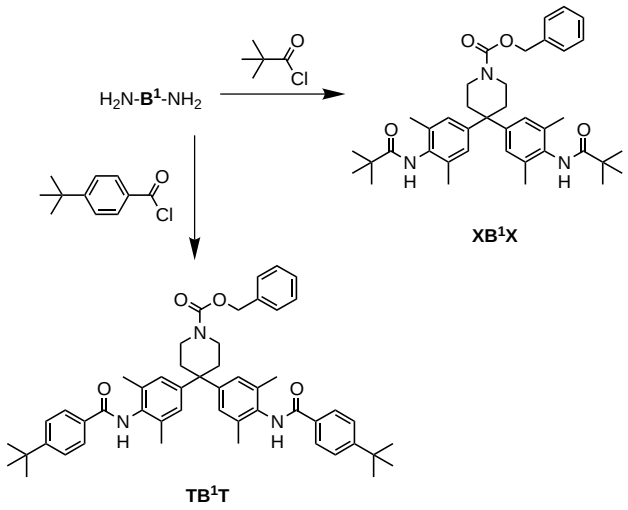

Scheme 2.

The components of the zipper complexes required for the (**AIB^{1}T**)$_2$ double-mutant cycle were prepared by using the routes shown in Schemes 3–5, below. Excess H_2N-**B^1**-NH_2 was treated with 4-*tert*-butylbenzoyl chloride and trimethylacetyl chloride to obtain **TB^1**–NH_2 and **XB^1**–NH_2 respectively after purification by column chromatography (Scheme 3). Monofunctionalised acid chloride **AI**–Cl was readily prepared from isophthaloyl chloride and 2,6-diisopropylaniline as described previously (Scheme 3),[37] but it proved impossible to obtain the *n*-hexyl analogue **HI**–Cl by this method. **AIB^{1}T** and **AIB^{1}X** were therefore obtained by direct coupling of **AI**–Cl with the appropriate monoamines **TB^1**–NH_2 and **XB^1**–NH_2 (Scheme 4). **HIB^{1}T** and **HIB^{1}X** were obtained by a different procedure. The appropriate monoamine, **TB^1**–NH_2 or **XB^1**–NH_2, was added to an excess of isophthaloyl chloride, the reaction was then quenched with excess *n*-hexylamine, and the products were separated by column chromatography (Scheme 5).

Similar methodology was used to obtain the components of the longer zippers based on **TBIBT·AIBIA**. Isophthaloyl chloride was added to excess

0947-6539/02/0823-5438 $ 20.00+.50/0 *Chem. Eur. J.* **2002**, *8*, No. 23

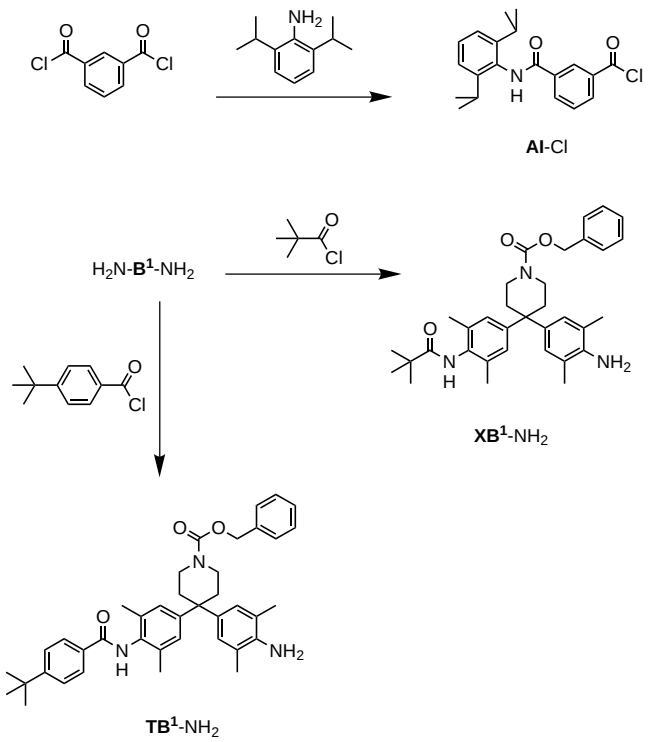

Scheme 3.

H_2N-**B**^{1}-NH_2, and the resulting amide oligomers were separated by column chromatography to give H_2N-**B**^{1}**IB**^{1}-NH_2 as the major product. This was then capped with an excess of 4-*tert*-butylbenzoyl chloride or trimethylacetyl chloride to give **TB**^{1}**IB**^{1}**T** and **XB**^{1}**IB**^{1}**X** respectively (Scheme 6). **AIB**^{2}**IA** was obtained directly by coupling the highly solubilised bisaniline H_2N-**B**^{2}-NH_2 with **AI**–Cl (Scheme 7). **HIB**^{2}**IH** was obtained adding H_2N-**B**^{2}-NH_2 to an excess of isophthaloyl chloride, quenching the reaction with excess *n*-hexylamine, and then separating the products by column chromatography (Scheme 7).

Binding studies: Formation of the zipper complexes was investigated by using ^{1}H NMR titrations and dilutions in $CDCl_3$ at room temperature. Dilution experiments with the shortest zippers showed that dimerisation is negligible for these systems (Table 1), and the complexes could therefore be characterised in straightforward manner by titration experiments. The association constants, K_a, and complexation-induced changes in chemical shift (CIS) are listed in Table 2. The CIS pattern is similar to that reported previously for the zipper complexes.[37] The signals due to the amide protons,

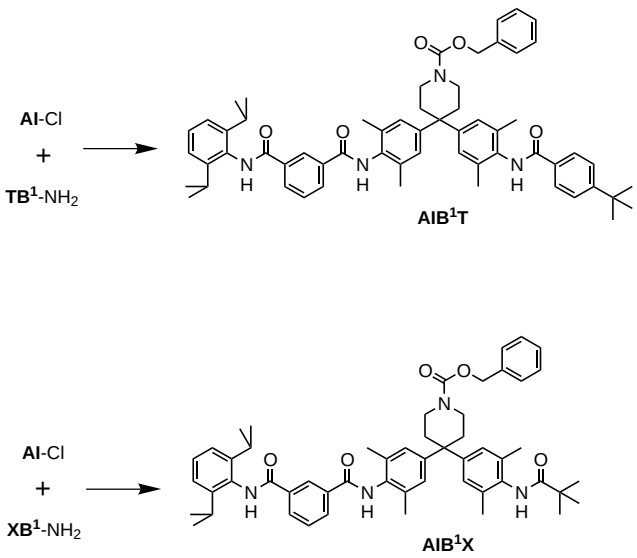

Scheme 4.

n, experience a downfield shift due to H bonding. The signals due to **t** and **d** on the **I** subunit experience large upfield shifts, while the signals due to **a** and **m** on the **B** subunit show small downfield shifts; this is characteristic of the edge-to-face interaction that docks **I** into the aromatic pocket of **B**. As reported previously, the **t** CIS value is lower in the **HIH** complexes, due to an increase in conformational flexibility relative to the **AIA** complexes.[38] In the **AIA** complexes, the geometry is locked by steric interactions with the isopropyl groups, but in the **HIH** complexes, the **I** subunit can flex to some extent inside the **B** binding pocket, and this produces large chemical-shift differences. However, this conformational difference has no impact on the analysis, because the thermodynamic effects on the core of the complex appear in both of the **HIH** complexes used in the double-mutant cycle, and they therefore cancel out.

The self-complementary (**AIB**^{1}**T**)$_2$ zippers were characterised by using dilution experiments; the dimerisation constants, K_d, and limiting CIS values are listed in Table 1. The CIS

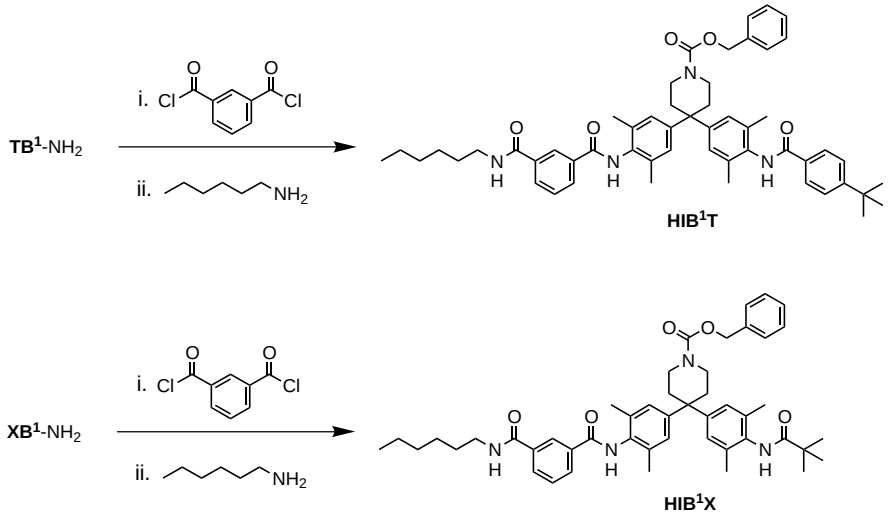

Scheme 5.

patterns are very similar to those observed in the shorter zippers. Intermolecular NOEs observed in ROESY experiments are listed in Table 3, and the proton-labelling scheme is given in Figure 6. These confirm that the complexes adopt the expected structures with interactions between the **B** and **I** subunits and between the terminal groups, **T**, **X**, **A** and **H**.

The longer zippers were more complicated systems to characterise. Dilution experiments showed that all of the compounds self-associate to a significant extent, and this equilibrium competes with the formation of the zipper complex. We found previously that these systems tend to form dimers rather than polymeric aggregates in solution.[37] The dilution experiments were therefore analysed by using a dimerisation model, but the self-association constants are not significantly different if an aggregation model is used. The dimerisation constants, K_d, and the CIS values are listed in Table 1. The dimerisation constants are an order of magnitude lower than the association constants for the formation of the **TBIBT·AIBIA** complexes, but the competing dimerisation equilibria broaden the ^{1}H NMR spectra and significantly complicate the analysis of titration experiments. These complexes were therefore studied by diluting 1:1 mixtures of the two components. This minimises the amount of dimer present throughout the experiment. The free chemical shifts of both species are known from the dilution experiments, and the K_a

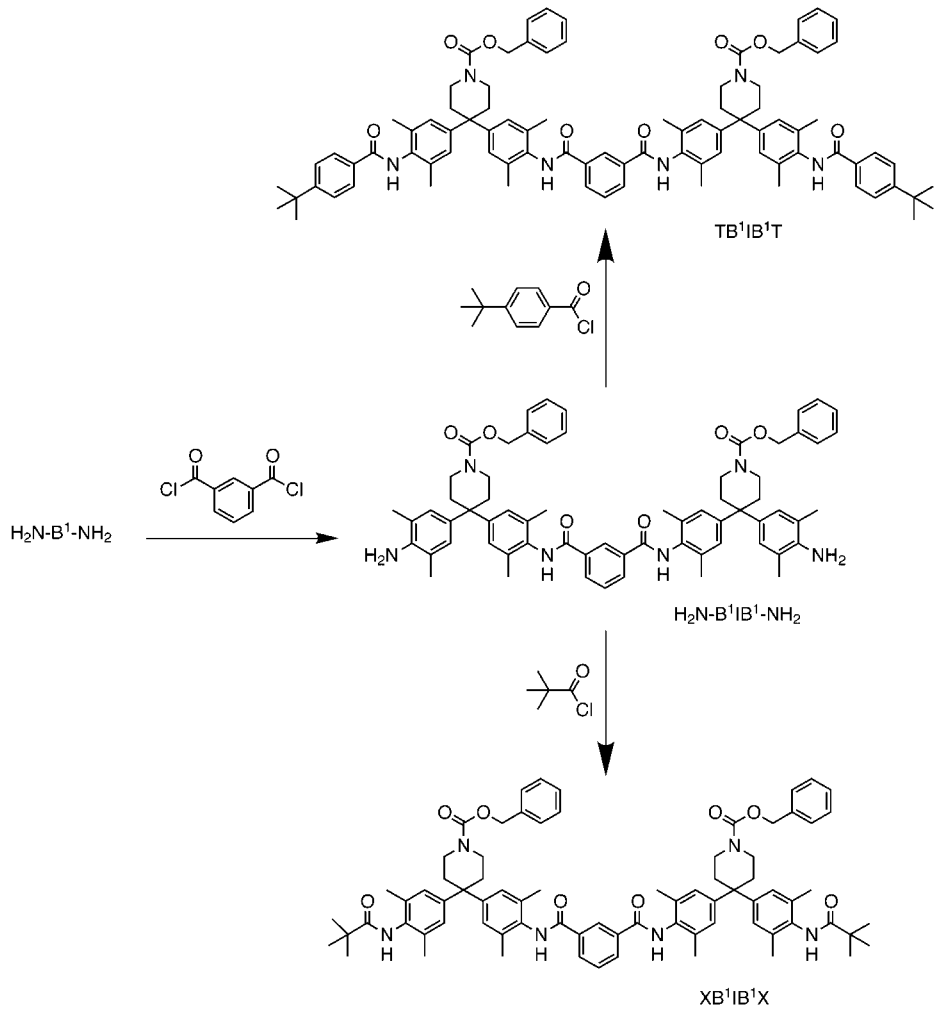

Scheme 6.

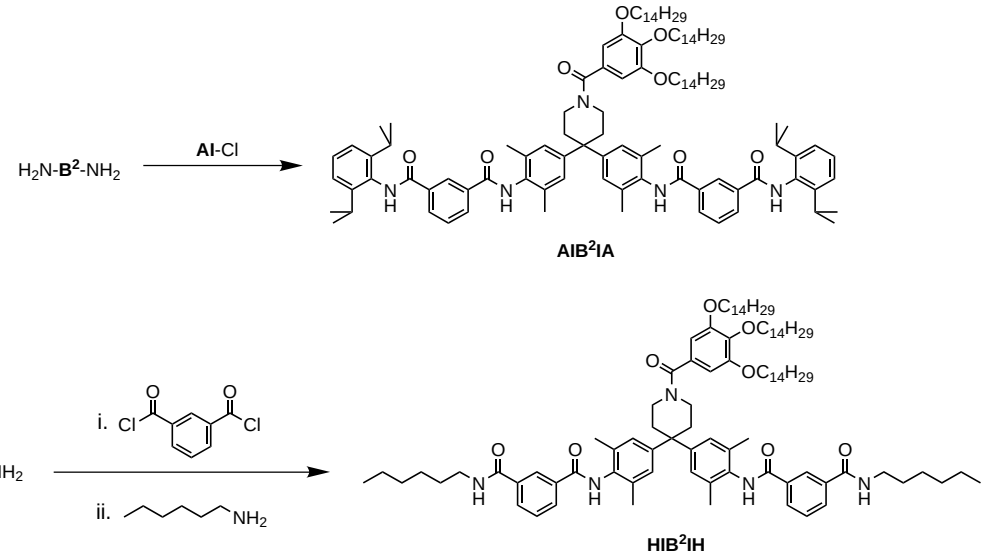

Scheme 7.

0947-6539/02/0823-5440 $ 20.00+.50/0 *Chem. Eur. J.* **2002**, *8*, No. 23

Table 1. Dimerisation constants, K_d [M^{-1}], and limiting dimerisation-induced changes in ^1H NMR chemical shift [ppm] in $CDCl_3$ at 298 K.[a]

		amides	**A/H** subunit		**I** subunit		**B** subunit		**T/X** subunit	
dimer	K_d	**n**	**h/i**	**j**	**t**	**d**	**a**	**m**	**e/f**	**g**
(**AIA**)$_2$	<1									
(**TB^{1}T**)$_2$	<1									
(**HIH**)$_2$	<1									
(**XB^{1}X**)$_2$	<1									
(**AIB^{1}T**)$_2$	210 ± 30	+1.7	−0.1	−0.2	−1.7	−0.5	+0.1[b]	−0.1[b]	−0.3	−0.5
		+1.3				−0.5				
		+1.2								
(**AIB^{1}X**)$_2$	39 ± 5	+1.6	−0.1	−0.1	−1.7	−0.6	+0.1[b]	−0.3	−0.3	
		+1.1				−0.4		−0.1		
		+0.7								
(**HIB^{1}T**)$_2$	49 ± 3	+1.6	−0.3		−1.0	−0.5	0.0	−0.3	0.0	−0.1
		+1.0				−0.3	−0.1	−0.1		
		+0.9								
(**HIB^{1}X**)$_2$	33 ± 5	+1.5	−0.3		−0.9	−0.5	0.0	−0.2	−0.1	
		+1.1				−0.3	−0.1	0.0		
		+0.5								
(**AIB^{2}IA**)$_2$	420 ± 40	+1.5	−0.1	−0.1	−1.3	−0.5	+0.2[b]	−0.1[b]		
		+0.7				−0.4				
(**TB^{1}IB^{1}T**)$_2$	81 ± 23	+1.5			−1.3	−0.5[b]	−0.1	−0.3	−0.1	−0.2
		+0.5					0.0	−0.2		
(**HIB^{2}IH**)$_2$	110 ± 30	+1.6	−0.3		−0.7	−0.3	0.0[b]	−0.2[b]		
		+1.0				−0.2				
(**XB^{1}IB^{1}X**)$_2$	150 ± 30	+1.4			−1.5	−0.6	0.0	−0.2[b]	−0.2	
		+0.4				−0.6	0.0			

[a] Errors in CIS are of the order of 20%. Where more than one proton was observed in each category, they are listed from the highest to the lowest CIS observed regardless of the position in the molecule. [b] Composite value for multiple unresolved signals. Protons not listed were unaffected by dimerisation (CIS $<$ 0.1).

Table 2. Association constants, K_a [M^{-1}], and limiting complexation-induced changes in ^1H NMR chemical shift [ppm] in $CDCl_3$ at 298 K.[a]

		amides	**A/H** subunit		**I** subunit		**B** subunit		**T/X** subunit	
complex	K_a	**n**	**h/i**	**j**	**t**	**d**	**a**	**m**	**e/f**	**g**[b]
titrations										
AIA · TB^{1}T	38 ± 2	+1.3	0.0	−0.1	−1.6	−0.4	+0.2	0.0	−0.3	−0.5
		+1.1								
AIA · XB^{1}X	6 ± 1	+1.3	0.0	−0.1	−1.5	−0.4	+0.1	0.0	−0.2	
		+0.5								
HIH · TB^{1}T	13 ± 1	+1.0	−0.3		−0.8	−0.3	0.0	0.0	+0.1	0.0
		+0.7								
HIH · XB^{1}X	6 ± 1	+1.2	−0.3		−0.9	−0.4	0.0	−0.1	[c]	
		+0.6								
dilutions										
AIB^{2}IA · TB^{1}IB^{1}T	10500 ± 980	[c]	0.0	−0.1	−1.7	−0.4[d]	+0.2	0.0	−0.3	−0.5
					−1.6		+0.1[d]	0.0		
								0.0		
AIB^{2}IA · XB^{1}IB^{1}X	1750 ± 90	+1.4	−0.1	−0.1	−1.7	−0.5[d]	+0.2	−0.1	−0.3	
		+1.4			−1.6		+0.2	−0.1		
		+1.1					+0.1	0.0		
		+0.8								
HIB^{2}IH · TB^{1}IB^{1}T	1850 ± 75	+1.4	−0.1		−1.6	−0.5	+0.1	−0.2	+0.1	0.0
		+1.4			−1.5	−0.5	+0.1	−0.1		
		+1.1				−0.4	0.0	−0.1		
		+1.1								
HIB^{2}IH · XB^{1}IB^{1}X	1000 ± 75	+1.7	−0.2		−1.5	−0.6	+0.1	−0.2	0.0	
		+1.0			−1.4	−0.5	+0.1	−0.1		
		+1.0				−0.4	0.0	0.0		
		+0.7								

[a] Errors in CIS are of the order of 20%. Where more than one proton was observed in each category, they are listed from the highest to the lowest CIS regardless of the position in the molecule. [b] Composite value for multiple unresolved signals. [c] These signals were not sufficiently resolved during the titration/dilution experiment to obtain reliable chemical-shift changes. Protons not listed were unaffected by complexation (CIS $<$ 0.1).

values are so large that the experiments start from almost 100% bound, so that the bound chemical shifts are also well-defined. Thus, the dilution data are analysed to determine one major unknown, K_a. The experiments were analysed with a model that also allowed for dimerisation of the two components by using the previously determined K_d and CIS values from Table 1. The results are listed in Table 2. The CIS values for formation of the **TBIBT · AIBIA** complexes show the

Table 3. Intermolecular NOEs observed in ROESY experiments in $CDCl_3$ at 298 K.

complex	core NOEs	terminal NOEs
$(\mathbf{AIB^1T})_2$	**t–m**, **d–a**, **d–m**	**j–f**, **j–g**, **k–o**, **l–o**
$(\mathbf{AIB^1X})_2$	**t–a**, **t–m**, **d–a**, **d–m**	
$(\mathbf{HIB^1T})_2$	**t–m**, **d–m**	
$(\mathbf{HIB^1X})_2$	**t–m**, **d–m**	**e–h**
$\mathbf{AIB^2IA \cdot TB^1IB^1T}$	**t–a**, **t–m**, **d–a**, **d–m**	**j–f**, **j–g**, **k–o**, **l–o**
$\mathbf{AIB^2IA \cdot XB^1IB^1X}$	**t–a**, **t–m**, **d–a**, **d–m**	
$\mathbf{HIB^2IH \cdot TB^1IB^1T}$	**t–a**, **t–m**, **d–a**, **d–m**	
$\mathbf{HIB^2IH \cdot XB^1IB^1X}$	**t–a**, **t–m**, **d–a**, **d–m**	

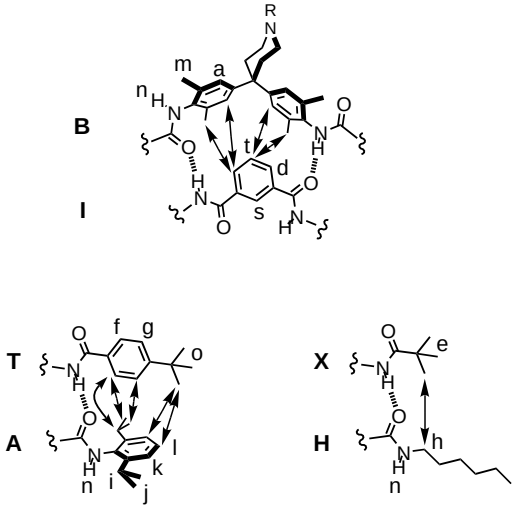

Figure 6. Representative NOEs observed in ROESY experiments. Each complex shows a subset of these NOEs as detailed in Table 3. The ^{1}H NMR labelling scheme and subunit nomenclature are also illustrated. The signals due to protons that are not labelled in this diagram are unaffected by complexation.

same pattern as the other two systems; this indicates that the expected zipper structure is obtained. This is supported by NOEs from ROESY experiments (Table 3).

Thus all of the complexes have similar structures and are suitable for the construction of double-mutant cycles and triple-mutant boxes. Table 4 summarises the stability-constant data from the titration and dilution experiments. When these values are used to construct double-mutant cycles, we find that, although the overall stability of the complexes varies by nearly three orders of magnitude, the sum of the two terminal $\mathbf{T \cdot A}$ interactions is similar in the all three systems (Figure 7). If we assume that the two $\mathbf{T \cdot A}$ interactions are identical, then

Table 4. Summary of stability constants, K [M^{-1}], free energies of binding, ΔG [kJ mol^{-1}], and double-mutant cycle interaction energies for the two terminal $\mathbf{T \cdot A}$ interactions, $\Delta\Delta G$ [kJ mol^{-1}].

complex	K	ΔG	$\Delta\Delta G$
$\mathbf{AIA \cdot TB^1T}$	38 ± 2	-8.9 ± 0.1	-2.6 ± 0.6
$\mathbf{AIA \cdot XB^1X}$	6 ± 1	-4.4 ± 0.4	
$\mathbf{HIH \cdot TB^1T}$	13 ± 1	-6.3 ± 0.2	
$\mathbf{HIH \cdot XB^1X}$	6 ± 1	-4.4 ± 0.4	
$(\mathbf{AIB^1T})_2$	210 ± 30	-13.1 ± 0.3	-3.1 ± 0.5
$(\mathbf{AIB^1X})_2$	39 ± 5	-9.0 ± 0.3	
$(\mathbf{HIB^1T})_2$	49 ± 3	-9.5 ± 0.1	
$(\mathbf{HIB^1X})_2$	33 ± 5	-8.5 ± 0.3	
$\mathbf{AIB^2IA \cdot TB^1IB^1T}$	$10\,500 \pm 980$	-22.6 ± 0.2	-2.9 ± 0.3
$\mathbf{AIB^2IA \cdot XB^1IB^1X}$	1750 ± 90	-18.2 ± 0.1	
$\mathbf{HIB^2IH \cdot TB^1IB^1T}$	1850 ± 75	-18.4 ± 0.1	
$\mathbf{HIB^2IH \cdot XB^1IB^1X}$	1000 ± 75	-16.9 ± 0.2	

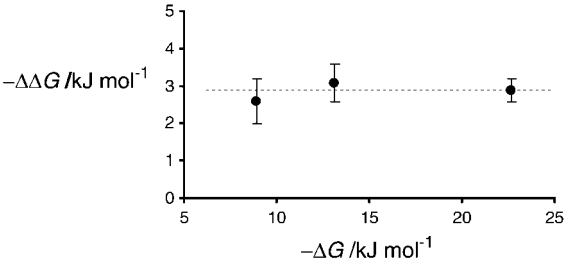

Figure 7. The sum of the two terminal $\mathbf{A \cdot T}$ interactions measured by using double-mutant cycles ($\Delta\Delta G$) plotted as a function of the overall stability of the zipper complex (ΔG). The dotted line corresponds to $\Delta\Delta G = -2.9$ kJ mol^{-1}, the mean interaction energy.

on average each $\mathbf{T \cdot A}$ interaction contributes -1.4 ± 0.2 kJ mol^{-1} to the overall stability of all of these complexes.[39] This value is identical to that determined previously in slightly different zipper complexes (-1.4 ± 0.5 kJ mol^{-1}).[35, 38] When we construct the triple-mutant boxes, the following results are obtained [Eqs. (4)–(6)].

$$\mathbf{TBT \cdot AIA} \rightarrow (\mathbf{AIBT})_2 \qquad \Delta\Delta G_{coop} = -0.5 \pm 0.8 \text{ kJ mol}^{-1} \qquad (4)$$

$$\mathbf{TBT \cdot AIA} \rightarrow \mathbf{TBIBT \cdot AIBIA} \qquad \Delta\Delta G_{coop} = -0.3 \pm 0.7 \text{ kJ mol}^{-1} \qquad (5)$$

$$(\mathbf{AIBT})_2 \rightarrow \mathbf{TBIBT \cdot AIBIA} \qquad \Delta\Delta G_{coop} = +0.2 \pm 0.6 \text{ kJ mol}^{-1} \qquad (6)$$

There is no detectable cooperativity in this system.

For these weak interactions (2.9 kJ mol^{-1}) in the zipper system, the magnitude of the enthalpic chelate effect lies within the experimental error (0.6–0.8 kJ mol^{-1}). Therefore, in double-mutant experiments over this range of complex stability ($\Delta G = 4$–23 kJ mol^{-1}), the effects of enthalpic cooperativity can be ignored, and free energy differences can be attributed to differences in functional-group interaction energies.[38]

Experimental evidence for enthalpic cooperativity in the vancomycin–peptide system is the large increase in limiting CIS values observed as the stability of the complex increases.[1, 3, 4, 20, 27] These chemical-shift changes are evidence for structural tightening related to a corresponding increase in the intrinsic functional-group interaction energy. In our experiments, we directly measure the functional-group interaction energies and see no differences in different zipper complexes. If we plot the limiting CIS values as a function of the overall stability of the complex, we also see no changes (Figure 8); that is, there is no structural tightening in this system, consistent with the thermodynamic measurements. Thus the zipper complexes described here appear to have very different properties from the vancomycin–peptide system reported by Williams, and further work is required to clarify the origins of this difference.

0947-6539/02/0823-5442 $ 20.00+.50/0 *Chem. Eur. J.* **2002**, *8*, No. 23

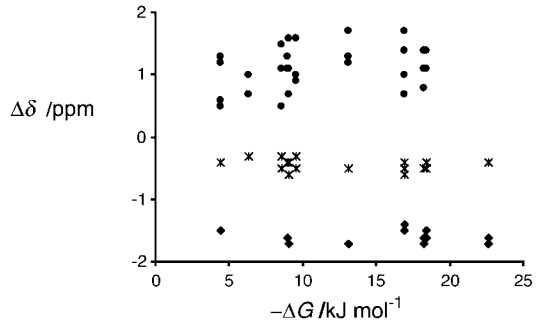

Figure 8. Complexation-induced changes in chemical shift (CIS) for the signals due to **n** (●), **d** (*) and **t** (◆) plotted as a function of the overall stability of the zipper complex (ΔG) (**t** data for the HI ··· complexes are not included as the values are perturbed by conformational flexibility as discussed in the text).

Conclusion

We have shown that triple-mutant boxes provide a powerful tool for experimentally investigating cooperativity in intermolecular interactions. Three double-mutant cycles have been constructed to quantify the same intermolecular functional group interaction in three different situations, in which the overall stability of the complexes varies by 13.7 ± 0.2 kJ mol^{-1}. The aromatic interaction we have quantified is worth -2.9 ± 0.5 kJ mol^{-1} in all three systems, and there is no detectable cooperative effect. Thus the simple additive approach used in our double-mutant cycle analysis of functional group interactions in the zipper complexes appears to be justified.

Experimental Section

The preparation of **AIA**, **HIH** and **AI**−Cl has been described previously.[37, 38] All other chemicals were purchased from Aldrich and used without further purification. The ^{1}H NMR signals are assigned by using the proton-labelling scheme in Figure 6.

Synthesis of 1: A mixture of 2,6-dimethylaniline (119 mL, 1.24 mol), *N*-acetyl-4-piperidone (55.4 mL, 0.45 mol) and concentrated hydrochloric acid (150 mL) was stirred under reflux. After 24 hours, more 2,6-dimethylaniline (13.1 mL, 0.12 mol) was added, and the same amount was added again after 48 hours. After a further 72 hours, the reaction mixture was cooled to room temperature and diluted with water (1.2 L). The resulting mixture was neutralised by addition of solid Na_2CO_3. The precipitate was then filtered off, washed with water (500 mL), Et_2O (500 mL) and pentane (500 mL) and dried under vacuum, yielding the desired product as a white powder (87.5 g, 60%). M.p. 203–205 °C; ^{1}H NMR (250 MHz, [D$_6$]DMSO, 21 °C): $\delta = 8.85$ (s, 1H; NH), 6.71 (s, 4H; ArCH), 4.41 (s, 4H; NH_2), 2.94 (m, 4H; CH_2NH), 2.40 (m, 4H; CH_2), 2.09 (s, 12H; Me); ^{13}C NMR (62.5 MHz, [D$_6$]DMSO, 21 °C): $\delta = 141.8$, 134.9, 127.8, 120.6, 115.9, 41.4, 41.1, 32.8, 18.22; MS (+ve, FAB): *m*/*z* (%): 324 (90) [M^+].

Synthesis of H_2N-B^1-NH$_2$: Compound **1** (14.14 g, 44 mmol) and Et_3N (9.13 mL, 66 mmol) were dissolved in MeOH (250 mL). A solution of benzyl chloroformate (6.87 mL, 48 mmol) in CH_2Cl_2 (30 mL) was added dropwise to the resulting suspension and the mixture was stirred for two hours. The volume of solvent was reduced by half under reduced pressure, and the mixture was poured into water (200 mL) and extracted with CH_2Cl_2 (3×100 mL). The organic layer was dried over Na_2SO_4 (anhydrous), evaporated under reduced pressure and then washed with pentane (500 mL), yielding the desired product as a pale yellow powder (13.6 g, 68% yield). M.p. 132–134 °C; ^{1}H NMR (250 MHz, $CDCl_3$, 21 °C): $\delta = 7.34$ (m, 5H; ArCH), 6.68 (s, 4H; **a**), 5.03 (s, 2H; OCH_2), 3.32 (s, 4H; NH_2), 2.48 (m, 4H; CH_2N), 2.14 (m, 4H; CH_2), 2.00 (s, 12H; **m**); ^{13}C NMR (62.5 MHz, [D$_6$]DMSO, 21 °C): $\delta = 154.7$, 141.7, 137.3, 134.8, 128.5, 127.9, 127.5, 126.1, 120.5, 66.10, 4.13, 4.12, 35.6, 18.2; MS (+ve, FAB): *m*/*z* (%): 457, (100) [M^++H]; elemental analysis calcd (%) for $C_{29}H_{34}N_3 \cdot \frac{1}{2}H_2O$: C 74.60, H 7.78, N 9.01; found: C 74.48, H 7.61, N 8.82.

Synthesis of 2: *n*-Propyl gallate (5.55 g, 26.2 mmol), 1-bromotetradecane (22 mL, 78.6 mmol) and anhydrous K_2CO_3 (32.22 g, 236 mmol) were suspended in acetone/DMSO (90:10, *v*/*v*; 100 mL). The mixture was stirred for 30 min at room temperature and then under reflux for 10 h. The reaction mixture was then poured into water (1.5 L), and the pH was brought to 6 with a mixture of HCO_2H/water (90:10, *v*/*v*). The product was extracted with CH_2Cl_2 (200 mL), and the organic layer was dried over Na_2SO_4 (anhydrous). The volume of solvent was reduced to 50 mL under reduced pressure, and the resulting solution was purified by flash column chromatography on basic alumina with CH_2Cl_2 as eluant. The resulting solid was suspended in a solution of KOH in EtOH/water (90:10, *v*/*v*; 0.5 M, 130 mL) and stirred for 1 h under reflux. The reaction was then cooled to room temperature and brought to pH 6 by adding a mixture of HCO_2H/water (90:10, *v*/*v*). The desired product precipitated upon addition of water (200 mL). It was filtered off, dried and recrystallised from hot EtOH and then dried under vacuum for 48 h (11 g, 56% yield). M.p. 43–45 °C; ^{1}H NMR (250 MHz, $CDCl_3$, 21 °C): $\delta = 7.31$ (s, 2H; Ar−CH), 4.02 (m, 6H; OCH_2), 1.81 (m, 6H; OCH_2CH_2), 1.47 (m, 6H; $OCH_2CH_2CH_2$), 1.25 (m, 60H; CH_2), 0.87 (t, 9H; Me); elemental analysis calcd (%) for $C_{49}H_{90}O_5$: C 77.52, H 11.95; found: C 77.87, H 12.12.

Synthesis of H_2N-B^2-NH$_2$: Oxalyl chloride (80 mL, 783 mmol) was added slowly to a suspension of acid **2** (6.6 g, 8.7 mmol) in CH_2Cl_2 (100 mL). The reaction mixture was stirred for 12 h, and then the solvent was removed under reduced pressure. To eliminate unreacted oxalyl chloride, the solid was dissolved in CH_2Cl_2 (100 mL), and the solvent was removed under reduced pressure. The last traces of oxalyl chloride were eliminated under high vacuum. The remaining solid was then dissolved in CH_2Cl_2 (40 mL) and added dropwise to a solution of **1** (2.5 g, 7.74 mmol) and Et_3N (1.63 mL, 11.6 mmol) in CH_2Cl_2 (40 mL), at 5 °C. The reaction mixture was stirred for 16 h at room temperature. The solution was then washed with aqueous HCl (1M, 200 mL) and aqueous NaOH (1M, 200 mL), and then dried with Na_2SO_4, filtered, and the solvent was removed under reduced pressure. Flash column chromatography on silica eluting with a mixture of CH_3Cl_2/EtOH (98:2, *v*/*v*) yielded H_2N-**B^2**-NH$_2$ as a white solid (5.34 g, 65% yield). M.p. 69–71 °C; ^{1}H NMR (250 MHz, $CDCl_3$, 21 °C): $\delta = 6.79$ (s, 4H; **a**), 6.52 (s, 2H; ArCH), 3.93 (t, 6H; OCH_2), 3.75 (m, 2H; CH_2N), 3.45 (m, 2H; CH_2N), 2.57 (m, 4H; CH_2), 2.20 (s, 12H; **m**), 1.75 (m, 6H; OCH_2CH_2), 1.43 (m, 6H; $OCH_2CH_2CH_2$), 1.25 (m, 60H; CH_2), 0.83 (t, 9H; Me); MS (+ve, FAB) *m*/*z* (%): 1066, (65) [M^++2H]; elemental analysis calcd (%) for $C_{70}H_{117}N_3O_4$: C 78.97, H 11.08, N 3.95; found: C 78.85, H 11.09, N 3.87.

Synthesis of TB^{1}T: 4-*tert*-butylbenzoyl chloride (1.52 mL, 7.8 mmol) was dissolved in CH_2Cl_2 (20 mL), and the mixture was cooled to 5 °C. H_2N-**B^1**-NH$_2$ (1.18 g, 2.6 mmol) and Et_3N (1.1 mL, 7.8 mmol) dissolved in CH_2Cl_2 (15 mL) were then added dropwise, and the resulting solution was stirred for 12 h at room temperature. Then CH_2Cl_2 (100 mL) was added, and the solution was washed with aqueous HCl (1M, 5×100 mL), aqueous NaOH (1M, 5×100 mL), water (200 mL) and brine (30 mL). The organic phase was dried over Na_2SO_4 (anhydrous), and the solvent was removed under reduced pressure. Recrystallisation from CH_2Cl_2/pet. ether (40–60) (50:50) yielded **TB^{1}T** as a white solid. (2.90 g, 97%). M.p. 250–252 °C; ^{1}H NMR (250 MHz, [D$_6$]DMSO, 21 °C): $\delta = 9.58$ (s, 2H; **n**), 7.91 (d, 4H; **f**), 7.52 (d, 4H; **g**), 7.34 (m, 5H; ArCH), 7.18 (s, 4H; **a**), 5.08 (s, 2H; OCH_2), 3.45 (m, 4H; CH_2N), 2.38 (m, 4H; CH_2), 2.13 (s, 12H; **m**), 1.28 (s, 18H; **o**); ^{13}C NMR (62.5 MHz, $CDCl_3$, 21 °C): $\delta = 165.7$, 155.4, 145.2, 136.8, 135.5, 132.0, 131.6, 128.5, 127.8, 127.2, 127.1, 126.9, 125.7, 67.0, 44.0, 41.0, 35.0, 31.2, 18.9. MS (+ve, FAB) *m*/*z* (%): 778 (100) [M^++H]; elemental analysis calcd (%) for $C_{51}H_{59}N_3O_4$: C 78.21, H 7.61, N 5.17; found: C 78.73, H 7.64, N 5.40.

Synthesis of XB^{1}X: Trimethylacetyl chloride (1.85 mL, 15 mmol) was dissolved in CH_2Cl_2 (20 mL), and the mixture was cooled to 5 °C. H_2N-**B^1**-NH$_2$ (2.3 g, 5 mmol) and Et_3N (2.1 mL, 15 mmol) in CH_2Cl_2 (50 mL) were then added dropwise. The solution was stirred for 12 h at room temperature. The product was isolated as a white powder after workup of the reaction by using the procedure described for **TB^{1}T**. **XB^{1}X** was obtained as a white solid (2.00 g, 66% yield). M.p. 237–239 °C; ^{1}H NMR (250 MHz, $CDCl_3$ 21 °C): $\delta = 7.33$ (m, 4H; ArCH), 6.88 (s, 4H; **a**), 6.80 (s, 2H; **n**), 5.10 (s, 2H; OCH_2), 3.52 (m, 4H; CH_2N), 2.28 (m, 4H; CH_2), 2.12 (s, 12H; **m**),

1.33 (s, 18H; **e**); ^{13}C NMR (62.5 MHz, $CDCl_3$, 21 °C): $\delta = 176.5$, 154.5, 145.0, 135.3, 131.9, 128.5, 127.9, 127.8, 126.8, 66.9, 44.0, 41.0, 39.3, 27.8, 18.7. MS (+ve, FAB) *m/z* (%): 626, (100) [M^+]; elemental analysis calcd (%) for $C_{39}H_{51}N_3O_4$: C 74.85, H 8.21, N 6.71; found: C 75.44, H 8.15, N 6.61.

Synthesis of XB^1–NH$_2$: A mixture of H_2N-**B^1**-NH_2 (11 g, 24 mmol) and Et_3N (5.0 mL, 36 mmol) in CH_2Cl_2 (60 mL) was cooled to 5 °C. Trimethylacetyl chloride (0.74 mL, 6 mmol) dissolved in CH_2Cl_2 (300 mL) was added dropwise over a period of 2 h. The solution was then allowed to warm up to room temperature and stirred for a further 12 h. The solution was then washed with aqueous HCl (1M, 10 × 100 mL), water (200 mL) and brine (30 mL). The organic phase was dried over Na_2SO_4 (anhydrous), and the solvent was removed under reduced pressure. Flash column chromatography with CH_2Cl_2 as eluant yielded **XB^1**–NH_2 as a white powder (3.19 g, 98% yield). M.p. 222–225 °C; ^{1}H NMR (250 MHz, [D$_6$]DMSO, 21 °C): $\delta =$ 8.60 (s, 1H; **n**), 7.38 (m, 5H; ArCH), 6.93 (s, 2H; **a**), 6.77 (s, 2H; **a**), 5.09 (s, 2H; OCH_2), 4.40 (s, 2H; NH_2), 3.43 (m, 4H; CH_2N), 2.18 (m, 4H; CH_2), 2.05 (s, 6H; **m**), 2.02 (s, 6H; **m**), 1.23 (s, 9H; **e**); ^{13}C NMR (62.5 MHz, [D$_6$]DMSO, 21 °C): $\delta = 176.4$, 155.0, 146.3, 142.4, 137.5, 135.6, 133.6, 133.4, 128.9, 128.3, 127.9, 126.6, 126.1, 120.9, 66.5, 43.1, 41.4, 35.7, 27.9, 18.7; MS (+ve, FAB) *m/z* (%): 541, (100) [M^+]; elemental analysis calcd (%) for $C_{34}H_{43}N_3O_3$: C 75.38, H 8.00, N 7.76; found: C 74.49, H 8.04, N 7.35.

Synthesis of TB^1–NH$_2$: **TB^1**–NH_2 was prepared in the same way as **XB^1**–NH_2, with H_2N-**B^1**-NH_2 (16.0 g, 35 mmol) and 4-*tert*-butylbenzoyl chloride (2.3 mL, 11 mmol). The desired product was obtained as a white solid (5.49 g, 81% yield) after flash column chromatography with CH_2Cl_2/MeOH (98:2, *v/v*) as eluant. M.p. 262–265 °C; ^{1}H NMR (250 MHz, [D$_6$]DMSO, 21 °C): $\delta = 9.53$ (s, 1H; **n**), 7.93 (d, 2H; **f**), 7.52 (d, 2H; d, **g**), 7.34 (m, 5H; ArCH), 7.03 (s, 2H; **a**), 6.78 (s, 2H; **a**), 5.07 (s, 2H; OCH_2), 4.42 (s, 2H; NH_2), 3.48 (m, 4H; CH_2N), 2.29 (m, 4H; CH_2), 2.16 (s, 6H; **m**), 2.02 (s, 6H; **m**), 1.32 (s, 9H; **o**); ^{13}C NMR (62.5 MHz, [D$_6$]DMSO, 21 °C): $\delta = 165.3$, 155.0, 154.7, 146.71, 142.4, 137.5, 135.6, 133.5, 133.2, 132.1, 128.9, 128.2, 127.9, 127.8, 126.6, 126.3, 125.6, 121.0, 66.5, 43.1, 41.4, 35.1, 31.4, 18.9, 18.7; MS (+ve, FAB) *m/z* (%): 618 (60) [M^++H].

Synthesis of AIB^{1}X: **XB^1**–NH_2 (0.638 g, 1.18 mmol) and Et_3N (0.210 mL, 1.47 mmol) were dissolved in CH_2Cl_2 (50 mL), and the mixture was cooled to 5 °C. Freshly prepared **AI**–Cl (0.506 g, 1.47 mmol) dissolved in CH_2Cl_2 (25 mL) was added dropwise. The reaction mixture was then stirred for 16 h at room temperature. The solution was washed with HCl (1M, 3 × 100 mL), water (200 mL) and brine (30 mL), the organic phase was dried over Na_2SO_4 (anhydrous), and the solvent was removed under reduced pressure. Flash column chromatography on silica (eluant CH_2Cl_2/EtOH 99.5:0.5, *v/v*) yielded **AIB^{1}X** as a white powder (0.88 g, 88% yield). M.p. 153–155 °C; ^{1}H NMR (250 MHz, $CDCl_3$ 21 °C): $\delta = 8.40$ (s, 1H; **s**), 8.22 (s, 1H; **n**), 7.86 (s, 1H; **n**), 7.77 (d, 1H; **d**), 7.73 (d, 1H; **d**), 7.34 (t, 1H; **t**), 7.38 (m, 5H; ArCH), 7.20 (t, 2H; **l**), 7.10 (s, 1H; **n**), 7.02 (d, 1H; **k**), 6.95 (s, 2H; **a**), 6.83 (s, 2H; **a**), 5.10 (s, 2H; OCH_2), 3.53 (m, 4H; CH_2N), 3.12 (m, 2H; **i**), 2.18 (m, 4H; CH_2), 2.10 (s, 6H; **m**), 2.05 (s, 6H; **m**), 1.17 (s, 9H; **e**), 1.02 (d, 12H; **j**); ^{13}C NMR (62.5 MHz, [D$_6$]DMSO, 21 °C): $\delta = 176.5$, 166.3, 165.3, 155.3, 147.7, 147.0, 146.5, 135.7, 135.6, 133.6, 133.0, 132.9, 131.1, 129.3, 128.9, 128.4, 128.2, 127.7, 126.9, 126.6, 126.1, 122.0, 66.7, 45.1, 36.0, 29.1, 28.2, 26.9, 24.6, 24.0, 23.3, 18.7, 18.6; HRMS (FAB) $m/z = 849.4907$, $C_{54}H_{65}N_4O_5^+$ requires 849.4955.

Synthesis of AIB^{1}T: **AIB^{1}T** was prepared in the same way as **AIB^{1}X**, starting from **TB^1**–NH_2 (0.67 g, 1.08 mmol) and **AI**–Cl (0.47 g, 1.35 mmol). **AIB^{1}T** was isolated as a white powder (0.97 g, 89% yield) after chromatography (eluant CH_2Cl_2/EtOH 99.5:0.5, *v/v*). M.p. 197–199 °C; ^{1}H NMR (250 MHz, [D$_6$]DMSO, 21 °C): $\delta = 9.85$ (s, 1H; **n**), 9.72 (s, 1H **n**), 9.55 (s, 1H; **n**), 8.48 (s, 1H; **s**), 8.16 (d, 1H; **d**), 8.08 (d, 1H; **d**), 7.87 (d, 2H; **f**), 7.66 (t, 2H; **t**), 7.49 (d, 2H; **g**), 7.38 (m, 5H; ArCH), 7.31 (t, 1H; **l**), 7.20 (d, 2H; **k**), 7.09 (s, 4H; **a**), 5.07 (s, 2H; OCH_2), 3.55 (m, 4H; CH_2N), 3.10 (m, 2H; **i**), 2.22 (m, 4H; CH_2), 2.13 (s, 6H; **m**), 2.08 (s, 6H; **m**), 1.33 (s, 9H; **o**), 1.20 (d, 12H; **j**); ^{13}C NMR (62.5 MHz, [D$_6$]DMSO, 21 °C): $\delta = 167.5$, 166.9, 164.3, 155.8, 154.7, 147.2, 146.9, 146.6, 136.9, 135.7, 135.6, 135.2, 134.8, 134.6, 133.7, 132.3, 132.1, 130.9, 128.9, 128.0, 127.5, 126.1, 124.2, 122.8, 45.7, 36.2, 31.5, 28.7, 26.0, 24.4, 24.0, 22.7, 18.7; HRMS (FAB) $m/z = 925.5229$, $C_{60}H_{69}N_4O_5^+$ requires 925.5268.

Synthesis of HIB^{1}X: **XB^1**–NH_2 (0.70 g, 1.30 mmol) and Et_3N (0.22 mL, 1.56 mmol) were dissolved in CH_2Cl_2 (100 mL) and added dropwise to a solution of isophthaloyl dichloride (5.28 g, 26 mmol) in CH_2Cl_2 (200 mL) at 5 °C. The solution was then stirred for 2 h at room temperature. After this period, the mixture was added dropwise to a solution of *n*-hexylamine (5.50 g, 52 mmol) and Et_3N (7.29 mL, 52 mmol) in CH_2Cl_2 (200 mL) at 5 °C. The resulting solution was stirred for 16 h at room temperature, and then washed with aqueous HCl (1M, 4 × 150 mL), aqueous NaOH (1M, 2 × 150 mL) and brine (2 × 50 mL). The organic phase was dried over Na_2SO_4 (anhydrous), and the solvent was removed under reduced pressure. Flash chromatography on silica eluting with a mixture of $CHCl_3$/EtOH (97.5:2.5, *v/v*) yielded **HIB^{1}X** as a white solid (0.48 g, 48% yield). M.p. 194–196 °C; ^{1}H NMR (250 MHz, $CDCl_3$, 21 °C): $\delta = 8.35$ (s, 1H; **s**), 8.07 (s, 1H; **n**), 7.90 (d, 1H; **d**), 7.68 (d, 1H; **d**), 7.33 (m, 5H; ArCH), 7.11 (t, 1H; **t**), 7.06 (s, 1H; **n**), 6.97 (s, 2H; **a**), 6.92 (s, 2H; **a**), 6.76 (s, 1H; **n**), 5.10 (s, 2H; OCH_2), 3.54 (m, 4H; CH_2N), 3.51 (m, 2H; **h**), 2.33 (m, 4H; CH_2), 2.18 (s, 6H; **m**), 2.12 (s, 6H; **m**), 1.77 (m, 2H; $NHCH_2CH_2$), 1.30 (m, 15H; **e**/CH_2), 0.84 (m, 3H; CH_3); ^{13}C NMR (62.5 MHz, [D$_6$]DMSO, 21 °C): $\delta = 175.6$, 167.0, 163.5, 154.7, 148.4, 147.4, 135.1, 134.9, 134.6, 132.6, 132.0, 130.0, 128.9, 128.4, 127.6, 127.5, 126.8, 126.3, 125.6, 66.3, 45.4, 41.0, 40.5, 31.9, 29.4, 27.5, 26.3, 22.8, 18.6, 18.4, 13.97; HRMS (FAB) $m/z = 773.4612$, $C_{48}H_{61}N_4O_5^+$ requires 773.4642.

Synthesis of HIB^{1}T: **HIB^{1}T** was prepared and purified in the same way as **HIB^{1}X**, starting from **XB^1**–NH_2 (0.80 g, 1.30 mmol). **HIB^{1}T** was obtained as a white solid (0.51 g, 46% yield). M.p. 180–182 °C; ^{1}H NMR (250 MHz, $CDCl_3$ 21 °C): $\delta = 8.31$ (s, 1H; **s**), 7.95 (s, 1H; **n**), 7.91 (d, 1H; **d**), 7.86 (d, 2H; **f**), 7.76 (d, 1H; **d**), 7.56 (s, 1H; **n**), 7.49 (d, 2H; **g**), 7.34 (m, 5H; ArCH), 7.15 (t, 1H; **t**), 7.01 (s, 2H; **a**), 6.97 (s, 2H; **a**), 6.61 (t, 1H; **n**), 5.11 (s, 2H; OCH_2), 3.45 (m, 4H; CH_2N), 3.38 (m, 2H; **h**), 2.33 (m, 4H; CH_2), 2.12 (s, 6H; **m**), 2.16 (s, 6H; **m**), 1.76 (m, 2H; $NHCH_2CH_2$), 1.34 (s, 9H; **o**), 1.29 (m, 6H; CH_2), 0.90 (m, 3H; CH_3); ^{13}C NMR (62.5 MHz, $CDCl_3$, 21 °C): $\delta = 166.5$, 166.0, 165.3, 155.2, 145.1, 144.8, 136.6, 135.6, 134.9, 134.4, 133.7, 132.3, 132.0, 130.1, 128.3, 127.8, 127.6, 127.1, 126.4, 126.3, 125.4, 66.9, 43.5, 40.8, 40.0, 35.5, 34.8, 31.3, 31.0, 29.3, 26.5, 22.4, 18.7, 18.5, 13.9; HRMS (FAB) $m/z =$ 849.4957, $C_{48}H_{61}N_4O_5^+$ requires 849.4955.

Synthesis of H$_2$N-B^{1}IB^1-NH$_2$: Isophthaloyl dichloride (0.93 g, 4.58 mmol) was dissolved in CH_2Cl_2 (85 mL), and the solution was added dropwise to a mixture of Et_3N (1.30 mL, 9.16 mmol) and H_2N-**B^1**-NH_2 (2.5 g, 4.6 mmol) in CH_2Cl_2 (150 mL). The resulting solution was stirred for 16 h, then the solvent was removed under reduced pressure. Flash chromatography on silica, with a gradient elution with a mixture $CHCl_3$/THF (98:2 to 90:10, *v/v*) allowed separation of unreacted H_2N-**B^1**-NH_2 from the desired H_2N-**B^{1}IB^1**-NH_2, which was obtained as a white powder (3.20 g, 67%). M.p. 231–233 C; ^{1}H NMR (250 MHz, [D$_6$]DMSO, 21 °C): $\delta = 9.83$ (s, 2H; **n**), 8.53 (s, 1H; **s**), 8.32 (d, 2H; **d**), 7.68 (t, 1H; **t**), 7.32 (m, 10H; ArCH), 7.05 (s, 4H; **a**), 6.80 (s, 4H; **a**), 5.08 (s, 4H; OCH_2), 4.38 (s, 4H; NH_2), 3.50 (m, 8H; CH_2N), 2.30 (m, 8H; CH_2), 2,16 (s, 12H; **m**), 2.08 (s, 12H; **m**); ^{13}C NMR (62.5 MHz, $CDCl_3$, 21 °C): $\delta = 165.3$, 154.7, 146.6, 142.0, 137.2, 135.2, 135.1, 133.1, 132.7, 130.2, 128.5, 127.8, 127.5, 127.0, 126.3, 125.9, 125.0, 120.7, 67.1, 66.2, 42.8, 35.4, 18.5, 18.2; MS (+ve, FAB) *m/z* (%): 1047 (100) [M^++H].

Synthesis of XB^{1}IB^{1}X: H_2N-**B^{1}IB^1**-NH_2 (2.97 g, 2.85 mmol) and Et_3N (0.85 mL, 6.27 mmol) were dissolved in CH_2Cl_2 (25 mL) and added dropwise to a solution of trimethylacetyl chloride (0.7 mL, 5.70 mmol) in CH_2Cl_2 (25 mL). The mixture was stirred for 16 h and then washed with aqueous HCl (1M, 5 × 100 mL), aqueous NaOH (1M, 5 × 100 mL), water (200 mL) and brine (50 mL). The organic layer was dried over anhydrous Na_2SO_4, and the solvent was removed under reduced pressure. Flash chromatography on silica eluting with CH_2Cl_2/EtOH (97:3, *v/v*) yielded the desired product (3.10 g, 90% yield). M.p. 206–207 °C; ^{1}H NMR (250 MHz, $CDCl_3$, 21 °C): $\delta = 8.70$ (s, 2H; **n**), 8.46 (s, 1H; **s**), 7.83 (s, 2H; **n**), 7.79 (d, 2H; **d**), 7.37 (m, 10H; ArCH), 7.05 (s, 4H; **a**), 6.95 (s, 4H; **a**), 6.50 (t, 1H; **t**), 5.08 (s, 4H; OCH_2), 3.50 (m, 8H; CH_2N) 2.25 (m, 8H; CH_2), 2.13 (s, 24H; **m**), 1.26 (s, 18H; **e**); ^{13}C NMR (62.5 MHz, $CDCl_3$, 21 °C): $\delta = 176.8$, 165.1, 147.2, 146.8, 135.0, 134.9, 133.6, 131.6, 131.5, 130.8, 128.8, 128.2, 127.9, 126.6, 125.6, 66.5, 45.1, 41.4,. 38.9, 35.9, 27.6, 18.6, 18.4; MS (+ve, FAB) *m/z* (%): 1213 (100) [M^++H]; elemental analysis calcd (%) for $C_{76}H_{88}N_6O_8$: C 75.22, H 7.31, N 6.92; found: C 75.92, H 7.41, N 6.80.

Synthesis of TB^{1}IB^{1}T: **TB^{1}IB^{1}T** was synthesised and purified in the same way as **XB^{1}IB^{1}X**, by using 4-*tert*-butylbenzoyl chloride (0.69 mL, 3.46 mmol), and H_2N-**B^{1}IB^1**-NH_2 (1.2 g, 1.16 mmol). **TB^{1}IB^{1}T** was obtained as a white powder (1.20 g, 76% yield). M.p. 250–252 °C; ^{1}H NMR (250 MHz, [D$_6$]DMSO, 21 °C): $\delta = 9.82$ (s, 2H; **n**), 9.58 (s, 2H; **n**), 8.50 (s, 1H; **s**), 8.25 (d, 2H; **d**), 7.91 (d, 4H; **f**), 7.72 (t, 1H; **t**), 7.52 (d, 4H; **g**), 7.33 (m, 10H; ArCH), 7.12 (s, 8H; **a**), 5.09 (s, 4H; OCH_2), 3.44 (m, 8H; CH_2N),

0947-6539/02/0823-5444 $ 20.00+.50/0 *Chem. Eur. J.* **2002**, *8*, No. 23

2.36 (m, 8H; CH_2), 2.15 (s, 12H; **m**), 2.11 (s, 12H; **m**), 1.30 (s, 18H; **o**); ^{13}C NMR (62.5 MHz, $CDCl_3$, 21 °C): $\delta = 165.7, 155.1, 147.4, 147.1, 135.1, 133.65, 131.6, 131.4, 128.9, 128.1, 127.8, 127.3, 127.0, 125.9, 66.4, 41.2, 35.7, 34.9, 31.1, 18.7, 18.5$. MS (+ve, FAB) m/z (%): 1363 (100) $[M^+ + H]$; elemental analysis calcd (%) for $C_{88}H_{96}N_6O_8 \cdot 2H_2O$: C 75.40, H 7.19, N 6.00; found: C 75.69, H 7.17, N 5.84.

Synthesis of AIB^{2}IA: H_2N-**B^2**-NH_2 (2.54 g, 2.38 mmol) and Et_3N (1.00 mL, 7.14 mmol) dissolved in CH_2Cl_2 (25 mL) were added dropwise to a solution of freshly prepared **AI**–Cl (2.46 g, 7.14 mmol) in CH_2Cl_2 (25 mL) at 5 °C. The solution was then stirred for 16 h at room temperature. The solvent was removed under reduced pressure. Flash chromatography by using a gradient elution with a mixture CH_2Cl_2/THF (98:2 to 90:10, *v*/*v*) yielded **AIB^{2}IA** as a white solid (0.80 g, 20% yield). ^{1}H NMR (250 MHz, [D_6]DMSO, 21 °C): $\delta = 8.82$ (s, 2H; **n**), 8.67 (s, 2H; **n**), 8.54 (s, 2H; **s**), 8.11 (d, 4H; **d**), 7.45 (t, 2H; **t**), 7.22 (t, 2H; **l**), 7.08 (d, 4H; **k**), 6.91 (s, 4H; **a**), 6.45 (s, 2H; ArCH), 3.85 (m, 6H; OCH_2), 3.71 (m, 4H; CH_2N), 3.06 (q, 4H; **i**), 2.57 (m, 4H; CH_2), 2.17 (s, 12H; **m**), 1.65 (m, 6H; OCH_2CH_2), 1.36 (m, 6H; $OCH_2CH_2CH_2$), 1.12 (m, 84H; CH_2/**j**), 0.76 (t, 9H; CH_3); ^{13}C NMR (62.5 MHz, $CDCl_3$, 21 °C): $\delta = 170.4, 166.1, 165.4, 153.2, 146.5, 145.0, 139.2, 136.3, 134.0, 133.8, 132.5, 131.2, 131.0, 130.8, 129.0, 128.6, 126.5, 125.9, 123.6, 105.4, 73.5, 69.2, 43.8, 31.9, 30.3, 29.7–29.4$ (CH_2 solubilising group), 28.9, 26.1, 23.6, 22.7, 18.9, 14.1; HRMS (FAB) $m/z = 1679.2267$, $C_{110}H_{160}N_5O_8^+$ requires 1679.2296.

Synthesis of HIB^{2}ICH: H_2N-**B^2**-NH_2 (1.5 g, 1.41 mmol) and Et_3N (0.40 mL, 2.82 mmol) were dissolved in CH_2Cl_2 (250 mL) and added dropwise to a solution of isophthaloyl dichloride (11.45 g, 56.4 mmol) in CH_2Cl_2 (100 mL) at 5 °C. The solution was then stirred for 2 h at room temperature. After this period, the resulting solution was added dropwise to a solution of *n*-hexylamine (11.40 g, 112.8 mmol) and Et_3N (15.82 mL, 112.80 mmol) in CH_2Cl_2 (300 mL) at 5 °C and then stirred for 16 h at room temperature. The solution was then washed with aqueous HCl (1M, 4 × 300 mL), aqueous NaOH (1M, 2 × 200 mL), and brine (2 × 75 mL). The organic phase was dried over anhydrous Na_2SO_4, and concentrated under reduced pressure. Flash column chromatography on silica by using a gradient elution with $CHCl_3$/EtOH (100:0 to 97.5:2.5, *v*/*v*) yielded **HIH** (17.5 g, 53 mmol) and the desired **HIB^{2}IH**, which was obtained as a white solid. (0.42 g, 22% yield). M.p. 53–56 °C; ^{1}H NMR (250 MHz, $CDCl_3$ 21 °C): $\delta = 8.35$ (s, 2H; **s**), 8.00 (s, 2H; **n**), 7.80 (d, 2H; **d**), 7.73 (d, 2H; **d**), 7.23 (t, 2H; **t**), 6.98 (s, 4H; **a**), 6.67 (t, 2H; **n**), 6.52 (s, 2H; ArCH),), 3.96 (t, 6H; OCH_2), 3.42 (m, 4H; CH_2N), 3.35 (q, 4H; **h**), 2.32 (m, 4H; CH_2), 2.18 (s, 12H; **m**), 1.75–1.50 (m, 10H; CH_2), 1.50–1.30 (m, 10H; CH_2), 1.25 (m, 68H; CH_2), 0.86 (t, 15H; CH_3); ^{13}C NMR (62.5 MHz, [D_6]DMSO, 21 °C): $\delta = 166.8, 165.7, 155.5, 145.2, 136.7, 135.9, 134.6, 133.9, 132.2, 130.4, 128.5, 128.0, 127.8, 126.3, 125.9, 67.1, 43.2, 40.2, 31.4, 32.9, 32.6, 22.5, 18.7, 14.0$; MS (+ve, FAB) m/z (%): 1527 (100) $[M^+ + H]$; elemental analysis calcd (%) for $C_{88}H_{96}N_6O_8$: C 77.07, H 9.97, N 4.59; found: C 76.70, H 10.03, N 4.39.

^{1}H NMR binding studies: The procedures used for the dilution and titration experiments have been described previously.[38] The association constants for the longer zipper complexes were determined by dilution of 1:1 mixtures, and the data was analysed by using purpose-written software on an Apple Macintosh microcomputer, *NMRDil HG HH GG*. This program requires a previous determination of the dimerisation parameters (K_d, δ_d and δ_f) for the two components and fits the data to a 1:1 binding isotherm, taking into account the dimerisation equilibria for both the host and guest. The method starts by assuming that $[HG] = 0$, so that Equations (7) and (8) can be solved exactly for [HH] and [GG]. These values of are then used to solve Equation (9) for [HG]. Equations (10) and (11) give the concentrations of free host [H] and free guest [G]. At this point, $[H] + [HH] + [HG] \neq [H]_0$, and $[G] + [GG] + [HG] \neq [G]_0$, so the value of [HG] from Equation (9) is used in Equations (7) and (8) to re-evaluate [HH] and [GG], and the procedure is carried out repetitively until $[H] + [HH] + [HG] = [H]_0$, and $[G] + [GG] + [HG] = [G]_0$. This allows the set of simultaneous equations to be solved for the concentrations of all species present.

$$[HH] = \frac{1 + 4K_{dH}([H]_0 - [HG]) - \sqrt{1 + 8K_{dH}([H]_0 - [HG])}}{8K_{dH}} \quad (7)$$

$$[GG] = \frac{1 + 4K_{dG}([G]_0 - [HG]) - \sqrt{1 + 8K_{dG}([G]_0 - [HG])}}{8K_{dG}} \quad (8)$$

$$[HG] = \frac{1 + K([G]_0 - [GG])([H]_0 - [HH]) - \sqrt{(1 + K([G]_0 - [GG])([H]_0 - [HH]))^2 - 4K^2([G]_0 - [GG])([H]_0 - [HH])}}{2K} \quad (9)$$

$$[H] = [H]_0 - 2[HH] - [HG] \quad (10)$$

$$[G] = [G]_0 - 2[GG] - [HG] \quad (11)$$

$$\delta_{obs} = \frac{[HG]}{[H]_0}\delta_b + \frac{[HH]}{[H]_0}\delta_d + \frac{[H]}{[H]_0}\delta_f \quad (12)$$

in which [HH] is the concentration of host dimer, [GG] is the concentration of guest dimer, K_{dG} is the guest dimerisation constant, K_{dH} is the host dimerisation constant and δ_d is the limiting bound chemical shift of the host dimer.[41]

All experiments were performed at least twice. The association constant for a single run was calculated as the mean of the values obtained for each of the signals followed during the titration weighted by the observed changes in chemical shift. The association constants from different runs were then averaged. Errors are quoted at the 95% confidence limits (twice the standard error). For a single run, the standard error was determined by using the standard deviation of the different association constants determined by following different signals.

Acknowledgements

We thank the BBSRC (S.T.), Roche Discovery Welwyn (P.T.), the University of Sheffield (P.T.) and the Lister Institute (C.A.H.) for funding.

[1] D. H. Williams, M. S. Westwell, *Chem. Soc. Rev.* **1998**, *27*, 57–63.
[2] S. Albeck, R. Unger, G. Schreiber, *J. Mol. Biol.* **2000**, *298*, 503–520.
[3] S. R. Griffiths-Jones, M. S. Searle, *J. Am. Chem. Soc.* **2000**, *122*, 8350–8356.
[4] D. H. Williams, A. J. Maguire, W. Tsuzuki, M. S. Westwell, *Science* **1998**, *280*, 711–714.
[5] G. Schreiber, A. R. Fersht, *J. Mol. Biol.* **1997**, *270*, 111–122.
[6] J. P. Mackay, U. Gerhard, D. A. Beauregard, R. A. Maplestone, D. H. Williams, *J. Am. Chem. Soc.* **1994**, *116*, 4573–4580.
[7] A. Horovitz, A. R. Fersht, *J. Mol. Biol.* **1992**, *224*, 733–740.
[8] A. Horovitz, A. R. Fersht, *J. Mol. Biol.* **1990**, *214*, 613–617.
[9] D. A. Bell, S. G. Diaz, V. M. Lynch, E. V. Anslyn, *Tetrahedron Lett.* **1995**, *26*, 4155–4158.
[10] N. Colocci, P. B. Dervan, *J. Am. Chem. Soc.* **1995**, *117*, 4781–4787.
[11] N. Colocci, M. D. Distefano, P. B. Dervan, *J. Am. Chem. Soc.* **1993**, *115*, 4468–4473.
[12] M. D. Distefano, P. B. Dervan, *Proc. Natl. Acad. Sci. USA* **1993**, *90*, 1179–1183.
[13] C. A. Hunter, D. H. Purvis, *Angew. Chem.* **1992**, 104, 779–782; *Angew. Chem. Int. Ed. Engl.* **1992**, *31*, 792–795.
[14] J. S. Lyndsey, *New J. Chem.* **1991**, *15*, 153–180.
[15] K. Onan, J. Rebek, T. Costello, L. Marshall, *J. Am. Chem. Soc.* **1983**, *105*, 6759–6760.
[16] R. B. Prince, J. G. Saven, P. G. Wolynes, G. S. Moore, *J. Am. Chem. Soc.* **1999**, *121*, 3114–3121.
[17] P. Groves, M. S. Searle, M. S. Westwell, D. H. Williams, *J. Chem. Soc. Chem. Commun.* **1994**, 1519–1520.
[18] A. P. Bisson, C. A. Hunter, *Chem. Commun.* **1996**, 1723–1724.
[19] A. Pfeil, J.-M. Lehn, *J. Chem. Soc. Chem. Commun.* **1992**, 838–840.
[20] M. S. Searle, G. J. Sharman, P. Groves, B. Benhamu, D. A. Beauregard, M. S. Westwell, R. J. Dancer, A. J. Maguire, A. C. Try, D. H. Williams, *J. Chem. Soc. Perkin Trans. 1* **1996**, 2781–2786.
[21] M. S. Searle, D. H. Williams, *J. Am. Chem. Soc.* **1992**, *114*, 10690–10697.
[22] W. P. Jenks, *Proc. Nat. Acad. Sci. USA* **1981**, *78*, 4046.
[23] W. P. Jenks, *Adv. Enzymol.* **1975**, *43*, 219–410.
[24] M. I. Page, *Chem. Soc. Rev.* **1973**, *2*, 295.

  0947-6539/02/0823-5445 $ 20.00+.50/0

[25] M. S. Searle, M. S. Wetswell, D. H. Williams, *J. Chem. Soc. Perkin Trans. 2* **1995**, *2*, 141.
[26] M. S. Westwell, M. S. Searle, J. Klein, D. H. Williams, *J. Phys. Chem.* **1996**, *100*, 16000 – 16001.
[27] D. H. Williams, T. F. Gale, B. Bardsley, *J. Chem. Soc. Perkin Trans. 2* **1999**, 1331 – 1334.
[28] M. S. Searle, S. R. Griffiths-Jones, H. Skinner-Smith, *J. Am. Chem. Soc.* **1999**, *121*, 11615.
[29] P. J. Carter, G. Winter, A. J. Wilkinson, A. R. Fersht, *Cell* **1984**, *38*, 835 – 840.
[30] G. K. Ackers, F. R. Smith, *Annu. Rev. Biochem.* **1985**, *54*, 597 – 629.
[31] L. Serrano, M. Bycroft, A. R. Fersht, *J. Mol. Biol.* **1991**, *218*, 465 – 475.
[32] G. Schreiber, A. R. Fersht, *J. Mol. Biol.* **1995**, *248*, 478 – 486.
[33] Y. Aoyama, M. Asakawa, H. Yamagishi, H. Toi, H. Ogoshi, *J. Am. Chem. Soc.* **1990**, *112*, 3145 – 3151.
[34] Y. Aoyama, M. Asakawa, Y. Matsui, H. Ogoshi, *J. Am. Chem. Soc.* **1991**, *113*, 6233 – 6240.
[35] H. Adams, F. J. Carver, C. A. Hunter, J. C. Morales, E. M. Seward, *Angew. Chem.* **1996**, 108, 1628 – 1631; *Angew. Chem. Int. Ed. Engl.* **1996**, *35*, 1542 – 1544.
[36] Y. Kato, M. M. Conn, J. Rebek, *J. Am. Chem. Soc.* **1994**, *116*, 3279 – 3284.
[37] A. P. Bisson, F. J. Carver, D. S. Eggleston, R. C. Haltiwanger, C. A. Hunter, D. L. Livingstone, J. F. McCabe, C. Rotger, A. E. Rowan, *J. Am. Chem. Soc.* **2000**, *122*, 8856 – 8868.
[38] F. J. Carver, C. A. Hunter, P. S. Jones, D. J. Livingstone, J. F. McCabe, E. M. Seward, P. Tiger, *Chem. Eur. J.* **2001**, *7*, 4854 – 4862.
[39] The magnitude of the aromatic interactions in this system are small. The experiments are carried out in chloroform, and desolvation presumably reduces the value from that expected from gas phase calculations[40] and experiments in water, where the hydrophobic effect makes an important contribution.[31] In addition, the interaction is sensitive to the nature of the substituents and the precise geometrical arrangement.[38]
[40] S. Tsuzuki, K. Honda, T. Uchimaru, M. Mikami, K. Tanabe, *J. Am. Chem. Soc.* **2002**, *124*, 104 – 112.
[41] The curve fitting programme is available from the author on request.

Received: January 11, 2002
Revised: July 16, 2002 [F3790]

  0947-6539/02/0823-5446 $ 20.00+.50/0